Use of Frequency Derivatives in the Three-Dimensional Full-Wave Spectral Domain Technique

Joseph E. Pekarek and Tatsuo Itoh, *Fellow, IEEE*

Abstract— **Rational function approximations are used to extrapolate the frequency response of the scattering coefficients of three-dimensional (3-D) structures. The rational functions are constructed by applying Padé approximation techniques to single frequency solutions of the currents and the derivatives of the currents with respect to frequency. The currents and current derivatives are computed using a modified spectral domain technique. The efficiency of the method, along with the direct determination of the poles and zeros of the transfer function, make the method well-suited for model-based parameter estimation (MBPE). Multiple-frequency-point Padé approximations are also investigated.**

I. Introduction

THE PASSIVE structure models used by current microwave circuit design CAD tools are required to cover a broad range of parameter values and frequency points. It is extremely difficult to obtain models for many passive structures that are accurate for all ranges and combinations of design parameters. An alternate approach to this problem is to use more specialized models that operate over a more narrow range of design parameters and frequencies. This approach involves the generation of passive models tailored to the particular technology that is used for the design. For example, monolithic microwave/millimeter wave integrated circuit (MMIC) design requires microstrip-type passive structures with a relative dielectric constant of 12.9 with a fixed or small set of dielectric substrate heights. For a particular group of designers, the frequency ranges of interest are often much more narrow than would be required by a general model. This restriction on the range of design parameters allows much more accurate models to be generated for more specialized design purposes. Since the possible sets of ranges for all the different technologies and frequency bands would entail an extremely large set of models, it is desirable to have a method for generating these models automatically using numerical electromagnetic simulation. In this paper a method for a generating pole-zero based models from electromagnetic simulations is presented.

The presented method determines the currents and the derivatives of the currents with respect to frequency using a modified spectral domain technique (SDT). The implementation of the method of moments using frequency derivative information has been demonstrated in [1]–[5] for free-space scattering problems. The method used in this work for determining the wideband frequency response from the single frequency response and its derivatives is very similar to the Cauchy method presented in [5]. The significant contribution of this work is the incorporation of frequency derivative information into the SDT. The extrapolation of the frequency response of a three-dimensional (3-D) structure from information computed at one or two frequency points is used to demonstrate the method. A related technique is asymptotic-waveform-evaluation (AWE) [6], where low-order rational functions are used to approximate circuit responses. In [1]–[6], efficient methods for determining the required derivatives are available, whereas the functional form of the SDT Green's functions requires an analytically complex frequency derivative evaluation.

In order to obtain the frequency derivative information in a computationally efficient manner, a database approach is used which is similar to the database approach described in [7] and [8] for the determination of the moment matrix. The general approach is extended to allow not only the generation of the moment matrix from the database, but also the derivatives of the moment matrix with respect to frequency. This allows the computationally expensive derivative computations to be performed once for a given substrate and enclosure configuration, and then the results can be used for later calculations of various structures that use the same substrate and enclosure.

The extrapolation of the frequency response provides wideband information from information at a single frequency point. The proposed method is particularly well-suited to the simulation of structures with sharp resonances in their frequency response. The computation of the current solution requires an $O(N^3)$ algorithm, while the computation of the derivatives of the current solution uses an $O(N^2)$ algorithm. An order of magnitude or more decrease in the analysis time required to determine the frequency response is not uncommon.

II. Basic Principles

A. Model-Based Parameter Estimation

The use of model-based parameter estimation (MBPE) in electromagnetics allows the approximation of the electromagnetic behavior by a mathematical model that is chosen to represent the underlying physics of the problem [9]. The application of the MBPE technique to the approximation of distributed circuit transfer functions is based on the premise

Manuscript received March 25, 1996.

J. Pekarek is with Applied Wave Research, Inc., Redondo Beach CA 90278 USA.

T. Itoh is with the University of California, Los Angeles, Los Angeles, CA 90032 USA.

Publisher Item Identifier S 0018-9480(96)08535-3.

that the desired N-port frequency response is well approximated by a rational function of the form [4]

$$S(f) \approx \frac{\sum_{i=0}^{M} a_i f^i}{\sum_{i=0}^{P} b_i f^i} = \frac{A(f)}{B(f)}. \tag{1}$$

To accurately describe the frequency response over the entire infinite bandwidth, the order of the numerator and denominator (M and P, respectively) would be infinite. However, a lower-order M and P can be used to provide an accurate approximation of the response in a more limited bandwidth.

B. Padé Approximation

The functional form for the current distribution on the surface of the conductors will be an analytic function of frequency. The N-port parameters computed directly from the current distributions will also be analytic functions with respect to frequency. The concept of analytic continuation allows expression of the desired frequency response as a Taylor's series expanded about a fixed frequency f_0. A truncated version of the Taylor series of the response is given by

$$S(f) \cong C(f) = \sum_{i=0}^{N} c_i (f - f_0)^i \tag{2}$$

where the coefficients c_i are found directly from the frequency derivatives evaluated at f_0. The number of terms in the series is $N+1$ where N is the number of frequency derivatives to be computed. The Padé approximation technique is a method for finding the coefficients of the rational function approximation in (2), such that the derivatives (also referred to as moments) of the rational function and the truncated Taylor series are equal at $f = f_0$ up to order N. A more thorough explanation and an implementation of the Padé technique is given in [10].

C. Spectral Domain Method

The method of solution for the electromagnetics problem is based on the spectral-domain method applied to 3-D circuits in a rectangular PEC enclosure filled with a planar, piecewise constant stratified media similar to the approach taken in [7], [8], and [11]. The currents on the conductors will be spatially discretized using rooftop basis functions for the x and y currents and rectangular cross-section current vias for z-directed currents as shown in Fig. 1.

D. Determination of Derivatives of Current Distribution

The spectral domain method leads to the following set of linear equations, where each Z^{uv} term represents a submatrix

$$\begin{bmatrix} Z^{xx} & Z^{xy} & Z^{xz} \\ Z^{yx} & Z^{yy} & Z^{yz} \\ Z^{zx} & Z^{zy} & Z^{zz} \end{bmatrix} \begin{bmatrix} J_x \\ J_y \\ J_{yz} \end{bmatrix} = \begin{bmatrix} E_x \\ E_y \\ E_z \end{bmatrix}. \tag{3}$$

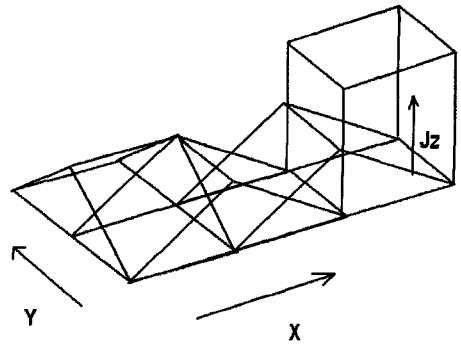

Fig. 1. Example current subsections.

An example entry for the submatrix Z^{xy} will be given as

$$Z_{pq}^{xy} = \sum_i \tilde{J}_{ypi} \tilde{J}_{xqi} \tilde{G}'_{xy_{i,pq}} \tag{4}$$

which expresses the coupling of basis p to basis q and the index i is a double index over the modes in the spectral domain. The transforms of the current basis given for the example above as $\tilde{J}_{ypi}$ and $\tilde{J}_{xqi}$ are constant with respect to frequency; hence, the derivatives of the moment matrix entries with respect to frequency can be found from

$$\frac{d^n Z_{pq}^{xy}}{df^n} = \sum_i \tilde{J}_{ypi} \tilde{J}_{xqi} \frac{d^n \tilde{G}'_{xy_{i,pq}}}{df^n} \tag{5}$$

which is seen to be identical to the moment matrix entry with the algebraic spectral domain Green's function replaced with its nth-order derivative. Consequently, the derivative of the moment matrix can be computed using the same database technique as is employed for the nondifferentiated moment matrix. Fast Fourier transforms (FFT's) are used to generate the databases for each dyadic Green's function component.

The solution of the SD equations will be expressed in the more compact notation as

$$[J] = [Z]^{-1}[E]. \tag{6}$$

For the determination of a rational function approximation, it is desired to find the derivatives of the current with respect to frequency. The differentiation can be generalized for nth-order differentiation as (similar to [4])

$$\frac{d^n[J]}{df^n} = -[Z]^{-1} \sum_{i=0 \cdots n-1} \binom{n}{i} \frac{d^{n-i}[Z]}{df^{n-i}} \frac{d^i[J]}{df^i} \tag{7}$$

which provides a recursive method of determining the higher-order derivatives of the current from the derivatives of the moment matrix found above. The computation of the nth-order current derivatives requires the derivatives of the moment matrix from order one to N.

E. Derivatives of Green's Functions

The algebraic spectral domain Green's functions need to be differentiated with respect to frequency, using an analytic differentiation procedure. The functional form for the planar Green's functions (x and y currents only) for a two layer

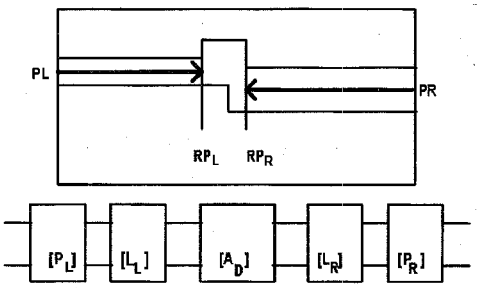

Fig. 2. De-embedding sections.

dielectric (a single substrate and air) configuration can be expressed as shown in (8) at the bottom of the page.

Differentiation of the Green's function with respect to frequency leads to a very complex expression. It can be shown that higher-order derivatives will lead to exponentially more complex computations as the order of the derivative increases. For this work, a maximum differentiation order of 12 will be used.

III. De-Embedding

Using the structure in Fig. 2 as an example, it is desired to find the scattering parameters of the structure from the reference plane at RP_L to the reference plane at RP_R. The excitation for the problem is applied as a gap voltage source at the edge of the enclosure at the ports PL and PR. The de-embedding procedure involves finding the solution (including the effects of port discontinuities and the feed lines) of the entire structure and its derivatives, and then removing the effects of the port discontinuities and feed lines. A differentiable de-embedding procedure allows the de-embedding of the solution and its derivatives directly, with the result being the solution and its derivatives for the de-embedded section of the structure.

The two-port problem is illustrated as shown in Fig. 2 where $[A_D]$ is the desired de-embedded chain matrix. The de-embedding chain matrices are given by

$$\begin{aligned}[D_L] &= [P_L][L_L] \\ [D_R] &= [L_R][P_R]\end{aligned} \tag{9}$$

where $[P_L]$ and $[P_R]$ are the port discontinuity chain matrices of the left and right ports, respectively, and $[L_L]$ and $[L_R]$ are the chain matrix representations of the uniform transmission line sections leading up to the desired reference planes. The de-embedding matrices for each port are computed from the results of the simulations of two de-embedding standards, where one standard is twice the length of the other as discussed in [7]. In a conventional de-embedding procedure, the chain matrix for the de-embedded section (designated $[A_d]$) is then found from

$$[A_d] = [D_L]^{-1}[A_t][D_R]^{-1} \tag{10}$$

where $[A_t]$ is the chain matrix of the entire structure.

For the differentiable de-embedding procedure, the chain matrix of the entire structure and all the computed higher-order derivatives of the entire structure are used in the de-embedding process. The term "derivatives" will be interpreted as the derivatives of a variable with respect to frequency, evaluated at a particular frequency. The chain matrix and its derivatives are given as $[A_t^{(n)}]$ where n is the order of the derivative. Similarly, the chain matrix and the computed higher-order derivatives of the inverse of the de-embedding sections will be given by $[(D_L^{-1})^{(n)}]$ and $[(D_R^{-1})^{(n)}]$. The de-embedded solution and the derivatives of the de-embedded solution are found from repeated application of the chain rule as demonstrated below

$$\begin{aligned}[A_d^{(0)}] &= [(D_L^{-1})^{(0)}][A_t^{(0)}][(D_R^{-1})^{(0)}] \\ [A_d^{(1)}] &= [(D_L^{-1})^{(1)}][A_t^{(0)}][(D_R^{-1})^{(0)}] + [(D_L^{-1})^{(0)}][A_t^{(1)}] \\ &\quad \cdot [(D_R^{-1})^{(0)}] + [(D_L^{-1})^{(0)}][A_t^{(0)}][(D_R^{-1})^{(1)}] \\ [A_d^{(2)}] &= \cdots \\ &\vdots \\ [A_d^{(n)}] &= \cdots.\end{aligned} \tag{11}$$

Once the chain matrix and the higher-order derivatives of the de-embedded solution are computed, any other port parameter (and its derivatives) can be found by application of standard differentiation rules to the port parameter transformations. A rational function approximation of the desired transfer function can then be found from the derivatives of the de-embedded solution.

IV. Sample Numerical Results

A. Meander Line

A point-by-point frequency simulation of the meandering line shown in Fig. 3 is compared to a MBPE simulation of the same structure. The response and the derivatives up to the 12th order at 9 GHz are used to determine a rational function with a sixth-order numerator and denominator. The results,

$$Z_{x/y,x/y}(f) = \frac{A}{\dfrac{\sqrt{f^2 - a_{nm}}}{f \cdot \tan\left(b_1\sqrt{f^2 - a_{nm}}\right)} + \dfrac{c_1\sqrt{\alpha f^2 - a_{nm}}}{f \cdot \tan\left(b_2\sqrt{\alpha f^2 - a_{nm}}\right)}} + \frac{B}{\dfrac{f}{\sqrt{f^2 - a_{nm}}\tan\left(b_1\sqrt{f^2 - a_{nm}}\right)} + \dfrac{c_2 f}{\sqrt{\alpha f^2 - a_{nm}}\tan\left(b_2\sqrt{\alpha f^2 - a_{nm}}\right)}} \tag{8}$$

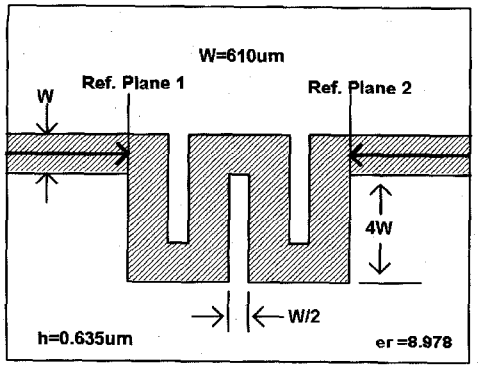

Fig. 3. Meander line structure from [11].

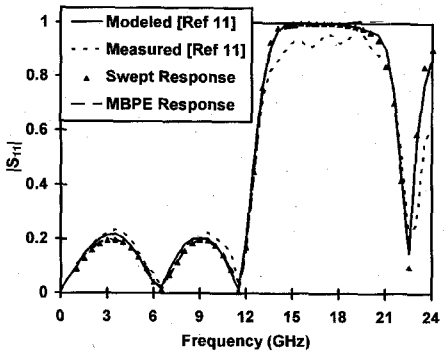

Fig. 4. Magnitude of S_{11} of meander line.

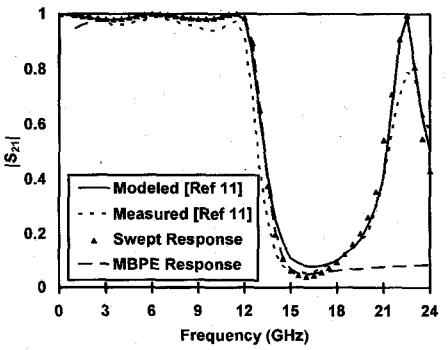

Fig. 5. Magnitude of S_{21} of meander line.

along with results and measured data from [11], are shown in Figs. 4 and 5.

The log of the error between the swept approach and the MBPE approach is shown in Fig. 6 for the magnitude and angle of S_{21}.

B. Spiral Inductor

A multiple-frequency-point Padé approximation will be used to determine the MBPE approximation of S_{22} for the spiral inductor shown in Fig. 7. The procedure for determining the multiple-frequency-point Padé approximation is very similar to the Cauchy method in [5]. The derivatives up to 12th order at the two expansion points are used to determine a rational function with a 12th-order numerator and a 13th-order denominator. The results of the de-embedded simulation will be compared to simulated and measured results in [12].

A comparison of the magnitude of S_{22} is shown in Fig. 8. The results from [12] are for an open substrate simulation,

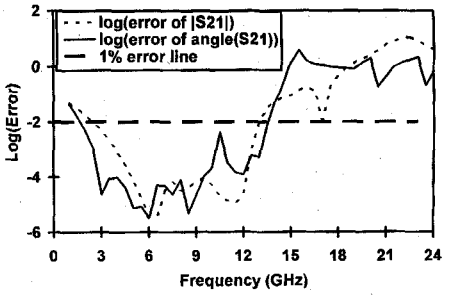

Fig. 6. Comparison of swept S_{21} to the MBPE of S_{21}.

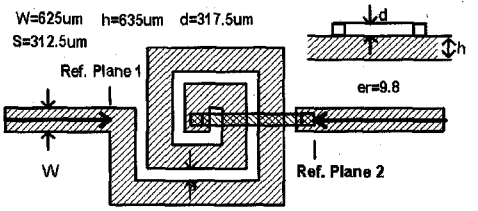

Fig. 7. Spiral inductor example from [12].

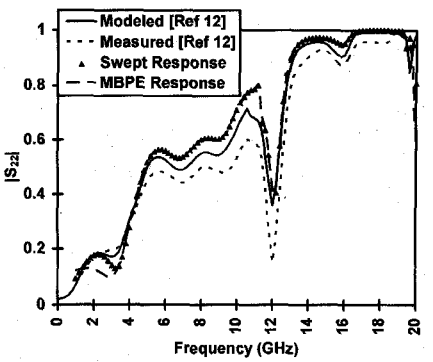

Fig. 8. Magnitude of S_{22} of spiral inductor.

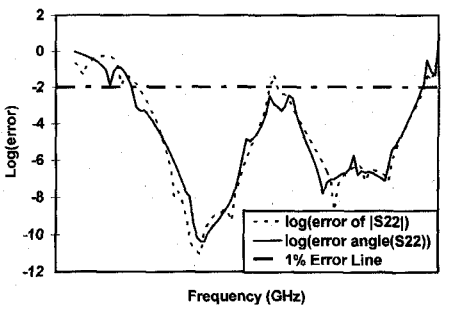

Fig. 9. Error for a multiple-frequency-point Padé approximation.

whereas the presented simulation method is for an enclosed substrate region. The difference between the presented simulation and the simulation from [12] can be attributed to the radiation loss from the open substrate simulation. The MBPE approximation was computed from the currents and their derivatives at both 8 GHz and 16 GHz. The difference between the MBPE solution and the point-by-point frequency swept solution is shown in Fig. 9.

C. Computation Times

The time required to compute the solution for each frequency point and the time required to compute the expan-

TABLE I
TIME COMPARISONS FOR MEANDER LINE ANALYSIS

	MBPE	*Point-by-Point (2, 2.5 ... 13 GHz)*
Database Generation / freq. point	5.1 min.	0.2 min.
Current Solve Time/ freq. point	13.7 min.	8.2 min.
Total Solution Time / freq. point	19 min.	8.6 min.
Total Database Computation	5.1 min.	4.6 min.
Total Current Solve Time	13.7 min.	188.6 min.
Total Solution Time	19 min.	197.8 min.

TABLE II
TIME COMPARISONS FOR SPIRAL INDUCTOR ANALYSIS

	MBPE	*Point-by-Point (4.6, 4.8 ... 19 GHz)*
Database Generation / freq. point	35.6 min.	0.73 min.
Current Solve Time/ freq. point	25. min.	15 min.
Total Solution Time / freq. point	61 min.	16 min.
Total Database Computation	71.2 min.	53.3 min.
Total Current Solve Time	50 min.	1095 min.
Total Solution Time	122 min.	1148.3 min.

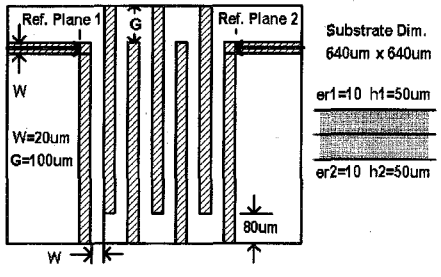

Fig. 10. Example Stripline Circuit.

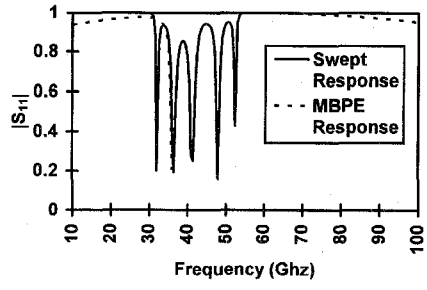

Fig. 11. S_{11} of stripline circuit (expansion frequency = 46 GHz).

sion for the MBPE at each frequency point are given along with total time comparisons for the swept responses in the frequency ranges where the errors are within one percent. The time required to compute the derivative database is listed separately since this computation only needs to be performed once for a given substrate/enclosure configuration and expansion frequency. For both the meander line and spiral simulations, the MBPE approach is shown to be about an order of magnitude faster than the point-by-point approach. If a precomputed derivative database is used, then the meander line computation time is 14 times faster, and the spiral computation time is 23 times faster.

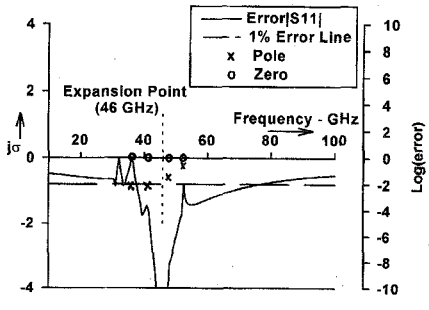

Fig. 12. Log(Error) in S_{11} for stripline circuit (expansion at 46 GHz).

V. BANDWIDTH ESTIMATION

A. Sample Circuit One

The example stripline circuit shown in Fig. 10 is used to study the behavior of the rational function approximations. The circuit has a frequency response with many close resonances. The simulated response for $|S_{11}|$ is shown in Fig. 11 for a point-by-point frequency sweep and an MBPE response. The expansion frequency is 46 GHz, and derivatives up to the 12th order are used to find a rational function with both the numerator and denominator of order six. The two responses are in very close agreement from about 37 GHz to about 75 GHz.

B. Accuracy Versus Expansion Frequency

The MBPE response of the example circuit shown in Fig. 10 is found for individual expansion points from 40 GHz to 51 GHz. For each expansion point, the MBPE response is found from the response and the derivatives up to the 12th order at the expansion point only. The graph shown in Fig. 12 shows the results for $|S_{11}|$ expanded about 46 GHz. The right y-axis of the graph shows the log of the error. The poles and zeros of the rational function are also shown on the same graph where the real x-axis is used as the imaginary frequency axis. The poles and zeros are shown on the same plot to demonstrate the connection between the accuracy of the MBPE response and the pole and zero locations.

A plot of the bandwidth of the approximation as a function of the expansion frequency is shown in Fig. 13. The bandwidth

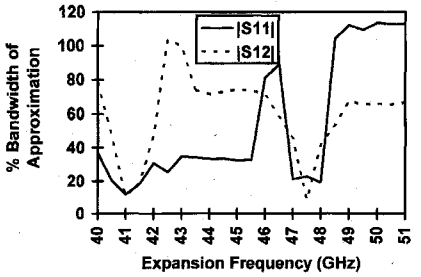

Fig. 13. Bandwidth of the rational function approximation.

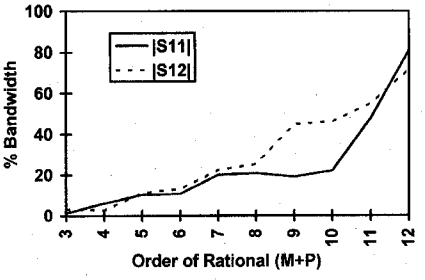

Fig. 14. Bandwidth of the rational function approximation.

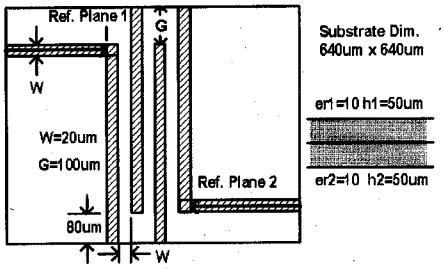

Fig. 15. Example stripline circuit-2.

is defined as

$$\text{bandwidth} = \frac{f_{\text{high}} - f_{\text{low}}}{f_{\text{expansion}}} \cdot 100\% \tag{12}$$

where f_{high} and f_{low} are the upper and lower bounds where the approximation is within one percent of the point-by-point frequency swept solution.

C. Accuracy Versus the Order of the Approximation

The order of the numerator (M) is set equal to the order of the denominator (P) or one less than the order of the denominator $(P-1)$. The order of the rational function is expressed as the sum of the orders of the numerator and the denominator $(P+M)$. The number of frequency derivatives used for the Padé approximation is equal to the order of the rational function $(M+P)$. The results are shown in Fig. 14.

D. Sample Circuit Two

The circuit shown in Fig. 15, referred to as circuit-2, is very similar to the previous stripline circuit except it has less resonant sections, which results in less poles and zeros in the same frequency band. Derivatives up to the 12th order at a single frequency are used to find a rational function with both the numerator and denominator of order six.

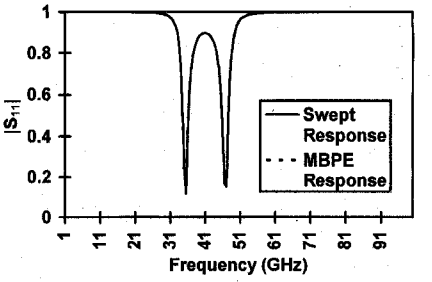

Fig. 16. S_{11} of stripline circuit-2 (expansion at 42 GHz).

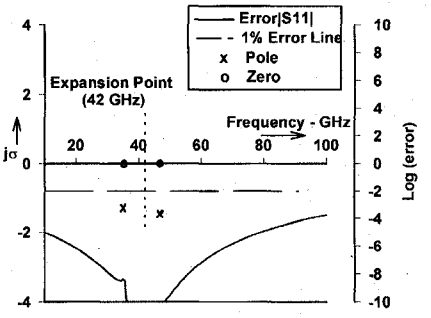

Fig. 17. Log (error) in s_{11} for stripline circuit-2 (expansion at 42 GHz).

The simulated response for $|S_{11}|$ is shown in Fig. 16 for a point-by-point frequency sweep and an MBPE response. The expansion frequency is 42 GHz. The two responses agree very well over the entire 1 GHz to 100 GHz bandwidth. The improved bandwidth results from fewer poles and zeros near the expansion point. The poles and zeros of circuit-2 are shown in Fig. 17 along with the error between the swept and MBPE responses.

VI. Conclusion

A method for determining the frequency response of 3-D microwave structures from information at a single frequency point was demonstrated. The principle advantages of the method are reduced computation times and the direct determination of the poles and zeros of the frequency response. The presented examples demonstrated "order of magnitude" decreases in computation times as compared to point-by-point frequency swept simulations. The direct determination of the poles and zeros eliminates the need for closely-spaced frequency points in a point-by-point swept frequency simulation. The method is capable of determining sharp resonances in the transfer function response that would possibly go unnoticed in a point-by-point simulation. The results show a definite connection between the accuracy of the rational function extrapolation and the positions of the poles and zeros of the transfer function relative to the expansion point.

References

[1] K. K. Kottapalli, T. K. Sarkar, Y. Hua, E. K. Miller, and G. J. Burke, "Accurate computation of wide-band response of electromagnetic systems utilizing narrow-band information," *IEEE Trans. Microwave Theory Tech.*, vol. 39, no. 4, pp. 682–687, Apr. 1991.

[2] K. Krishnamoothy, T. K Sarkar. and X. Yang, "Use of frequency-derivative information to reconstruct the scattered electric field of a

conducting cylinder over a wide frequency band," *J. Electromagn. Waves Applicat.*," vol. 5., no. 6, pp. 653–663, 1991.
[3] E. Arvas and X. Yang, "Use of frequency derivatives in computing the electromagnetic response of targets," in *Proc. 1990 Bilkent Int. Conf. New Trends in Communication, Control, and Signal Processing*, July 1990, pp. 596–599.
[4] X. Yang and E. Arvas, "Use of frequency derivative information in 2-dimensional electromagnetic scattering problem," in *IEE Proc. Microwave, Antennas and Propagat.*, Aug. 1991, pp. 269–272.
[5] R. S. Adve and T. K. Sarkar, "Generation of accurate broadband information from narrowband data using the Cauchy method," *Microwave Optical Technology Lett.*, vol. 6, no. 10, pp. 569–573, Aug. 1993.
[6] X. Huang, V. Raghavan, and R. A. Roher, "AWEsim: A program for the efficient analysis of linear(ized) circuits," in *Tech. Dig. IEEE Int. Conf. Computer-Aided Design*, 1990, pp. 534–537.
[7] A. Hill and V. K. Tripathi, "An efficient algorithm for the three-dimensional analysis of passive microstrip components and discontinuities for microwave and millimeter-wave integrated circuits," *IEEE Trans. Microwave Theory Tech.*, vol. 39, no. 1, pp. 83–91, Jan. 1991.
[8] J. C. Rautio and R. F. Harrington, "An electromagnetic time-harmonic analysis of shielded microstrip circuits," *IEEE Trans. Microwave Theory Tech.*, vol. MTT-35, no. 8, pp. 726–729, Aug. 1987.
[9] E. K. Miller and G. J. Burke, "Some applications of model-based parameter estimation in computational electromagnetics," in *Modern Antenna Design Using Computers and Measurements: Application to Antenna Problems of Military Interest*, AGARD Lecture Series no. 165, Oct. 1989, pp. 4.1–4.26.
[10] W. H. Press, S. A. Teukolsky, W. T. Vettering, and B. P. Flannery, *Numerical Recipes in C: The Art of Scientific Computing*, 2nd ed. Cambridge, MA: Cambridge Univ. Press, 1992, pp. 200–203.
[11] W. Wertgen and R. H. Jansen, "Efficient direct and iterative electrodynamic analysis of geometrically complex MIC and MMIC structures," *Int. J. Numerical Modeling: Electron. Networks, Devices and Fields*, vol. 2, pp. 153–186, 1989.
[12] T. Becks and I. Wolff, "Analysis of 3-D metallization structures by full-wave spectral domain technique," *IEEE Trans. Microwave Theory Tech.*, vol. 40, no. 12, Dec. 1992.

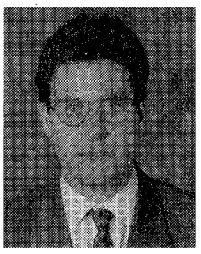

Joseph E. Pekarek received the B.S. degree in electrical engineering from South Dakota School of Mines and Technology, Rapid City, in 1988, the M.S. degree in electrical engineering from California State University, Northridge, in 1991, and the Ph.D. degree in electrical engineering from the University of California, Los Angeles, in March 1996.

He was with Hughes Aircraft Company, El Segundo, CA, from 1988 to 1994 as a MMIC and MIC Designer. He is currently President of Applied Wave Research, Inc., Redondo Beach, CA, which develops microwave CAD software. His research interests are in the area of fast methods for both electromagnetic analysis and microwave circuit simulation.

Tatsuo Itoh (S'69–M'69–SM'74–F'82), received the Ph.D. degree in electrical engineering from the University of Illinois, Urbana, in 1969.

From 1966 to 1976, he was with the Department of Electrical Engineering, University of Illinois. From April 1976 to August 1977, he was a Senior Research Engineer, Radio Physics Laboratory, SRI International, Menlo Park, CA. From August 1977 to June 1978, he was an Associate Professor at the University of Kentucky, Lexington. In July 1978, he joined the faculty at The University of Texas at Austin, where he became a Professor of Electrical Engineering in 1981 and Director of the Electrical Engineering Research Laboratory in 1984. During the summer of 1979, he was a Guest Researcher at AEG-Telefunken, Ulm, West Germany. In September 1983, he was selected to hold the Hayden Head Centennial Professorship of Engineering at The University of Texas. In September 1984, he was appointed Associate Chairman for Research and Planning of the Department of Electrical and Computer Engineering, The University of Texas. In January 1991, he joined the University of California, Los Angeles (UCLA), as Professor of Electrical Engineering and holder of the TRW Endowed Chair in Microwave and Millimeter Wave Electronics. He is currently Director of Joint Services Electronics Program (JSEP) and is also Director of Multidisciplinary University Research Initiative (MURI) program at UCLA. He was an Honorary Visiting Professor at Nanjin Institute of Technology, China and at Japan Defense Academy. In April 1994, he was appointed as Adjunct Research Officer for Communications Research Laboratory, Ministry of Post and Telecommunication, Japan. He currently holds Visiting Professorship at University of Leeds, United Kingdom. He has more than 215 journal publications, 370 refereed conference presentations in the area of microwaves, millimeter-waves, antennas, and numerical electromagnetics, and supervised more than 32 Ph.D. students.

Dr. Itoh is a member of the Institute of Electronics and Communication Engineers of Japan, and Commissions B and D of USNC/URSI. He served as the Editor of IEEE TRANSACTIONS ON MICROWAVE THEORY AND TECHNIQUES for 1983–1985. He serves on the Administrative Committee of IEEE Microwave Theory and Techniques Society. He was Vice President of the Microwave Theory and Techniques Society in 1989 and President in 1990. He was the Editor-in-Chief of IEEE MICROWAVE AND GUIDED WAVE LETTERS from 1991–1994. He was elected as an Honorary Life Member of MTT Society in 1994. He was the Chairman of USNC/URSI Commission D from 1988 to 1990, the Vice Chairman of Commission D of the International URSI for 1991–93 and is currently Chairman of the same Commission. He serves on advisory boards and committees of a number of organizations including the National Research Council and the Institute of Mobile and Satellite Communication, Germany.